Resilient Collision-tolerant Navigation in Confined Environments

Paolo De Petris[1,2], Huan Nguyen[1,2], Mihir Kulkarni[1], Frank Mascarich[1], and Kostas Alexis[1,2]

***Abstract*— This work presents the design and autonomous navigation policy of the Resilient Micro Flyer, a new type of collision-tolerant robot tailored to fly through extremely confined environments and manhole-sized tubes. The robot maintains a low weight (< 500g) and implements a combined rigid-compliant design through the integration of elastic flaps around its stiff collision-tolerant frame. These passive flaps ensure compliant collisions, contact sensing and smooth navigation in contact with the environment. Focusing on resilient autonomy, capable of running on resource-constrained hardware, we demonstrate the beneficial role of compliant collisions for the reliability of the onboard visual-inertial odometry and propose a safe navigation policy that exploits both collision-avoidance using lightweight time-of-flight sensing and adaptive control in response to collisions. The robot further realizes an explicit manhole navigation mode that exploits the direct mechanical feedback provided by the flaps and a special navigation strategy to self-align inside manholes with non-straight geometry. Comprehensive experimental studies are presented to evaluate, both individually and as a whole, how resilience is achieved based on the robot design and its navigation scheme.**

I. INTRODUCTION

Aerial robots are being utilized in an ever-increasing set of applications including inspection [1, 2] and surveillance [3]. Despite the progress, multiple essential environments still present unique challenges for autonomous entry and navigation of flying robots. This particularly relates to extremely confined settings commonly found in industrial or natural environments such as narrow manholes, ship ballast water tanks, and cave passages. Despite the availability of miniaturized flying platforms, autonomous operation in most such environments is yet to be achieved. The limited relevant demonstrated results utilize the benefits of collision-tolerant platforms [4] but have been constrained to manually piloted operations. Manual flight eliminates the need for reliable odometry estimation, safe planning, and robust autonomy in such conditions. However, this is in stark contrast with the potential aerial robots could have if enabled to navigate autonomously in important confined facilities in the energy and maritime industries, underground mines and more.

In response to the above needs and challenges, in this work we present a new collision-tolerant micro flying robot that combines rigid and compliant components and further integrates resilient navigation functions that explicitly account for the collision-tolerance of the platform and the interplay between collisions and onboard odometry estimation. This new robot called the Resilient Micro Flyer (RMF), is a lightweight (< 500g), small (0.32m-diameter), collision-tolerant system with its mechanical resilience realized through a combination of rigid and compliant components. Specifically, its rigid airframe core is combined with compliant "flaps" for softer collisions and contact sensing.

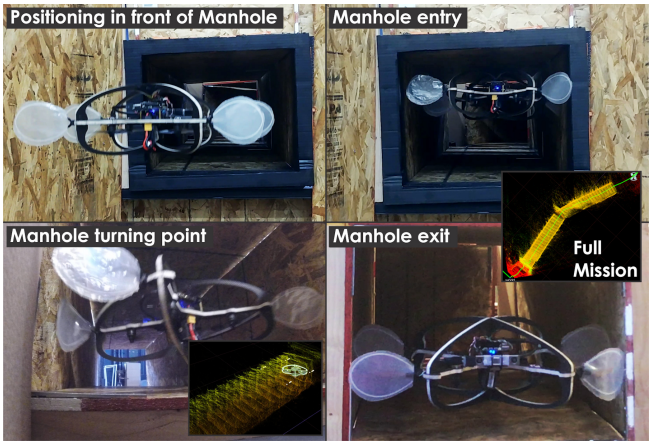

Fig. 1. RMF in a mission of autonomous manhole navigation.

To facilitate resilient autonomy in extremely confined environments such as manholes and obstacle-filled narrow corridors, RMF implements a navigation policy that not only utilizes visual-inertial odometry estimation and lightweight Time-Of-Flight (TOF) range sensors but also accounts for and exploits its collision-tolerance and compliant flaps to maximize the robot survivability. First, this relates to detecting collisions by flex-force sensors embedded inside the contact flaps. As the survivability of the onboard visual-inertial odometry estimation is sensitive to the magnitude of the collision forces, RMF benefits from compliant collisions and exploits its capability to sense impacts in order to adjust its forward acceleration such that collision events tend to lead to more conservative and thus safer navigation. Building on top of this collision-aware policy, RMF further utilizes its TOF sensors to reactively avoid as many of the obstacles in its environment as possible. These two policies have a synergistic role, while both enhance the likelihood of the visual-inertial solution to remain reliable. Furthermore, RMF emphasizes and implements explicit functionality for manhole navigation. This involves the detection of manhole openings, the automatic entry and flight through non-straight manholes by exploiting the role of the compliant flaps.

To evaluate the potential of RMF and its lightweight resilient navigation solution we present a set of experiments.

This material is based upon work supported by a) the Defense Advanced Research Projects Agency (DARPA) under Agreement No. HR00111820045, and b) the NSF award No. 2008904. The presented content and ideas are solely those of the authors.

This work was conducted while all the authors were with the University of Nevada, Reno, 1664 N. Virginia, 89557, Reno, NV, USA.

[1] University of Nevada, Reno, 1664 N. Virginia, 89557, Reno, NV, USA.

[2] NTNU, O. S. Bragstads Plass 2D, 7034, Trondheim, Norway. pdepetris@nevada.unr.edu

First, we demonstrate the ability of RMF to autonomously detect and navigate a 0.5×0.4m-wide and 5.2m-long manhole that involves a yaw turn. Second, we present the safe navigation of a narrow corridor filled with both large and thin obstacles. Subsequently, we present an explicit demonstration of the role of collisions-aware control adaptation. Last, we demonstrate the robustness of the elastic flaps-supported visual-inertial odometry in consecutive collision events.

The remainder of this paper is organized as follows: Section II presents related work, followed by the system description in Section III. The resilient navigation functionalities are presented in Section IV. Evaluation studies are detailed in Section V, followed by conclusions in Section VI.

II. RELATED WORK

A niche community of researchers has investigated the domain of collision-tolerant aerial robots. The work in [4] presents collision-tolerant Micro Aerial Vehicles (MAVs) implementing a rigid rolling cage. A similar design has been commercialized, while a set of other rigid commercial platforms exist. Our team has utilized such a design, albeit in a prototype form, in the autonomous exploration work conducted for the DARPA Subterranean Challenge [5]. Furthermore, our previous works involved collision-tolerant flying robots [6–8]. A much smaller collision-tolerant system was presented in [9]. Following a different principle of design, the authors in [10] detail a MAV with Euler spring-based compliant collision tolerance. The AirBurr robot, presented in [11], implements a ducted-fan system surrounded by a protective structure. While most such systems are rotorcrafts, the authors in [12] and [13] propose, respectively, a fixed-wing and blimp collision-tolerant design. Inspired by the body structure of insects and the relevant role of elastic proteins (e.g., resilin), the paper in [14] presents a collision resilient elastic quadrotor design. A study on the effects of the force applied to the external protective system on the robot has been conducted in [15]. A hybrid rolling-flying collision-tolerant platform was proposed in [16] and used in [17] exploiting the detected collisions. Exploiting a learning-based approach, another collision-based method is presented in [18]. An overview of collision-tolerant designs is available in [19]. The research presented in this work differs as on one hand we examine a robot implementing combined rigid and compliant collision-tolerance and on the other we focus on the interplay between mechanical tolerance and survivable autonomy. We outline both the design of a miniaturized, less than 500g, rigid-compliant collision-tolerant robot and the algorithms for its resilient autonomy.

III. SYSTEM DESIGN

This section provides an overview of the design of the Resilient Micro Flyer, outlining its rigid-elastic collision-tolerant frame, alongside its sensing and processing solution enabling resilient navigation through confined environments.

A. Resilient Micro Flyer Airframe

The design of RMF, depicted in Figure 2, focuses on collision-tolerance, prolonged endurance, and lightweight structure, which in turn further benefits the previous two goals. Resilient collision-tolerance is facilitated through the combination of a main rigid frame, alongside a set of compliant contact flaps detailed in the next subsection. The main rigid component of the collision-tolerant frame is fabricated through carbon-balsa sandwich material (total width equal to 6.35mm with 1mm carbon on each side, density: $0.316\text{g}/\text{cm}^2$) leading to a total airframe weight of 96g. The frame design of RMF is tailored to keeping the weight low, ensuring collision-tolerance across all dimensions and especially against lateral impacts, while some limited risk-zone exists on the front and back. The latter represents a trade-off for the purposes of maximizing the camera's unobstructed field-of-view. Regarding its propulsion, RMF integrates four T-Motor F1507 3800KV DC brushless motors controlled through electronic speed controllers. Finally, RMF integrates a PixRacer R15 as its low-level autopilot unit offering attitude and thrust control. High-level position control and autonomous navigation is facilitated through a separate ARM-based multi-core processor as detailed further in this section. The total weight of RMF, including all the sensing and processing components and its battery is 495g.

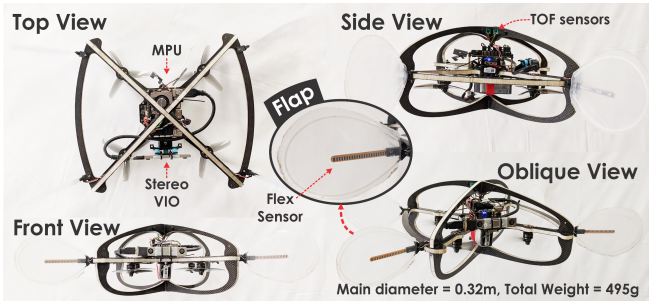

Fig. 2. RMF top, side, front, and oblique views.

B. Compliant Contact Flaps and Touch Sensing

Despite the fact that the implemented rigid collision-tolerant frame can mechanically sustain the expected forces of collisions, there is an experimentally-verified strong correlation between the forces of an impact and the survivability of the onboard visual-inertial odometry estimation process. A viable alternative is possible if the rigid collision-tolerant core of the design is combined with compliant components. This exceeds the integration of a rubber mount for the visual-inertial sensor to the main body, which is also part of the design. RMF further integrates passive flaps to facilitate compliant contact as depicted in Figure 2. The flap mechanisms are implemented through elastic nylon material with a thickness of 3.1mm leading to a total weight of only 3g per flap. The tensile strength of the selected material is 77.2-84.8MPa and its impact strength is 32-74.7J/m. A nylon sleeve is then attached around the main flap structure provided by the nylon rod. These durable flaps, enduring forces much stronger than those the robot experiences during collisions or intentional persistent physical interaction, facilitate more stable navigation in extremely confined environments, alongside robustifying the survivability of the onboard state estimation

as preliminarily indicated in Figure 3. Having a total length of 10cm and being able to fully bend by 90 degrees, they only marginally increase the robot size when fully bent, while ensuring passive reaction, self-centering in narrow tube-like settings and overall safer collision-tolerant navigation. In a manhole, for example, where the turbulence typically leads the robot to experience continuous collisions, thus possibly hindering its localization performance, the elastic flaps allow smooth traversal by ensuring almost continuous soft contact. The above is particularly driven by our experience on the effects of collisions on the onboard visual-inertial odometry both in the framework of this work but also through earlier studies with purely rigid collision-tolerant frames [5, 6, 20].

At the same time, the developed flaps integrate touch sensing capabilities. In particular, as depicted in Figure 2, the flap integrates a 5.5cm flex sensor that offers angle displacement measurement. It bends and flexes physically with the flap and its resistance changes from a nominal value of 10K Ohms to a minimum of twice that value at 180deg pitch bend as a function of the flap bending angle. The change is sensed by calibrated analog to digital converters onboard the high-level processing board of RMF.

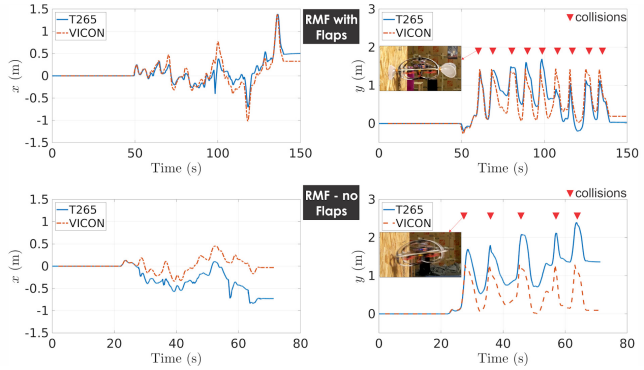

Fig. 3. Beneficial effect of the RMF compliant flaps in achieving resilient localization. With the flaps, the visual-inertial odometry (T265) closely follows VICON even post-collisions, whereas without, it quickly drifts.

C. High-Level Sensing and Processing Payload

The sensing payload of RMF is tailored to the goal of resilient autonomy in confined environments, while maintaining a lightweight configuration. RMF integrates a Realsense T265 tracker delivering visual-inertial odometry based on its onboard ASIC implementation and simultaneously allows processing its stereo fisheye camera pair and IMU data. The sensor provides informative data in illumination conditions as low as 15lux. By first subsampling the image to half of its size and then running the Semi Global Block Matching (SGBM) algorithm in [21], a reliable depth map is calculated and the respective point cloud is derived. Four miniaturized Time-Of-Flight sensors are integrated (each weighting < 1g) perimetrically around the robot, at $[45, 135, -45, -135]^\circ$ angles, for accurate ranging in the $[0.05, 2.5]$m range. Simultaneously, a micro 10m-range TOF sensor is integrated facing down on the robot. Moreover, the IMU data of the onboard autopilot are also interfaced. Last, the flex-force sensors on the two front flaps are interfaced. The above are all processed by the integrated Main Processing Unit (MPU) based on the Khadas VIM3 offering 4 A311D Cortex-A73 cores at 2.2GHz paired with 2 Cortex-A53 cores at 1.8GHz (big-little architecture). This board is responsible for the sensor processing and control tasks onboard RMF. The total sensors and MPU weight is limited to 91g.

D. Battery Module

The battery modules of RMF are custom-assembled through the combination of three 18650 Li-Ion High-Drain battery cells of 3.7V and 3120mAh connected in series. The selected high-drain batteries allow up to 30A of continuous current and 40A current bursts. The total weight of this 3-cell custom battery is 146g, a mass comparable to a standard 3S LiPo, but with double the energy density. Equipped with this battery solution, RMF presents an endurance of 14min.

IV. RESILIENT AUTONOMOUS NAVIGATION

Alongside the resilient design of RMF, a survivable and computationally-lightweight navigation strategy is designed which specifically accounts for the collision-tolerance of the platform and the interplay between collisions and robustness in onboard localizability. The overall policy for resilient navigation relies on a set of modes for a) safe navigation in confined and obstacle-filled environments through reactive collision-avoidance (Section IV-B) and collisions-aware adaptive control (Section IV-C), as well as b) manhole-sized openings traversal through automated manhole detection and fly-through navigation policy (Section IV-D). Specific details are provided below, alongside an overview of the position and yaw control onboard RMF.

A. Position and Yaw Control

Let $\mathcal{I}$ be the inertial frame, and $\mathcal{V}$ the yaw-rotated inertial frame. The position controller of RMF is a straightforward implementation of fixed-gain PID control while the yaw controller utilizes a proportional control scheme. This scheme works efficiently despite its simple control structure. Its efficacy for RMF is attributed to the nature of its rigid body dynamics and also the very fast and high dynamic range actuators utilized alongside its minimized weight. The outputs of the position and yaw controllers are the commanded acceleration vector expressed in $\mathcal{I}$, $[{}^{\mathcal{I}}a_r^x, {}^{\mathcal{I}}a_r^y, {}^{\mathcal{I}}a_r^z]$, and yaw rate $\dot{\psi}_r$ which are then converted to the attitude-thrust command, as per [22], and forwarded to the low-level controller inside the autopilot:

$$
\begin{aligned}
{}^{\mathcal{I}}a_r^x &= K_P^x(x_r - x) + K_I^x \int (x_r - x)dt\big|_{I_{\min}^x}^{I_{\max}^x} + K_D^x(\dot{x}_r - \dot{x}) \quad (1)\\
{}^{\mathcal{I}}a_r^y &= K_P^y(y_r - y) + K_I^y \int (y_r - y)dt\big|_{I_{\min}^y}^{I_{\max}^y} + K_D^y(\dot{y}_r - \dot{y})\\
{}^{\mathcal{I}}a_r^z &= K_P^z(z_r - z) + K_I^z \int (z_r - z)dt\big|_{I_{\min}^z}^{I_{\max}^z} + K_D^z(\dot{z}_r - \dot{z})\\
\dot{\psi}_r &= K_P^\psi(\psi_r - \psi)
\end{aligned}
$$

where $[x_r, y_r, z_r, \psi_r], [x, y, z, \psi]$ are the reference and estimated position and yaw angle of the robot, respectively expressed in $\mathcal{I}$; $I_{\min}^j, I_{\max}^j,\ j \rightarrow x, y, z$ are the saturation minimum and maximum values of the control integrals.

B. Reactive Collision Avoidance

RMF integrates and utilizes four 1D TOF sensors that provide reliable ranging in the immediate vicinity of the robot. Based on these sensors, RMF implements a last-resort lightweight reactive collision avoidance strategy which aims to avoid obstacles or, at the very least, tends to reduce the likelihood (and risks) of a forcible collision. Let $\delta_{FL}, \delta_{FR}, \delta_{RL}, \delta_{RR}$ be the distance values returned by the front-left, front-right, rear-left, rear-right TOF sensors, respectively. The implemented reactive avoidance policy takes the form of super-imposed acceleration commands added into the overall control policy as presented below:

$$\begin{aligned} {}^{\mathcal{V}}a_r^{x,a} &= {}^{\mathcal{V}}a_r^{x} + K_{ax}(\delta_F - \delta_B) \\ {}^{\mathcal{V}}a_r^{y,a} &= {}^{\mathcal{V}}a_r^{y} + K_{ay}(\delta_L - \delta_R) \end{aligned} \tag{2}$$

where $\delta_F = \delta_{FL} + \delta_{FR}$, $\delta_B = \delta_{RL} + \delta_{RR}$, $[\delta_L, \delta_R] = [\delta_{FL}, \delta_{FR}]$ if the robot moves forward, or $[\delta_{RL}, \delta_{RR}]$ if the robot moves backward, ${}^{\mathcal{V}}a_r^x, {}^{\mathcal{V}}a_r^y$ are the control commands computed in Eq. (1) expressed in $\mathcal{V}$, K_{ax}, K_{ay} are positive gains and ${}^{\mathcal{V}}a_r^{x,a}, {}^{\mathcal{V}}a_r^{y,a}$ are the updated acceleration references expressed in $\mathcal{V}$ given the effect of this reactive avoidance strategy. Here we utilize the estimated x-axis velocity in $\mathcal{V}$ of the robot to check if it is going forward or backward.

C. Collision-aware Adaptive Navigation

RMF is designed in view of the possibility that navigation in extremely confined environments with multiple and complex objects can lead to situations where collisions are unavoidable. In order to both best avoid collisions and mitigate their risks as much as possible, RMF implements an additional functionality beyond that of reactive avoidance using TOF sensing. Through the compliant contact flaps implementing touch sensing based on the flex sensors, RMF can detect collisions with its environment. As a collision can lead to disturbance to the desired trajectory and thus further subsequent oscillatory flight, while in addition a collision-event may imply that the rest of the environment is also collision prone, RMF implements a policy for collision-aware adaptive navigation. In particular, given the desired forward acceleration ${}^{\mathcal{V}}a_r^{x,a}$ calculated from Eq. (2), this is then automatically adjusted based on the following formula:

$$\begin{aligned} {}^{\mathcal{V}}a_{ad}^{x,a} &= k_c\, {}^{\mathcal{V}}a_r^{x,a},\ k_c = \frac{1}{N_c + 1} \\ N_c &= \min(N_c, N_c^{\max}),\quad N_c \leftarrow 0 \text{ if } t_k - t_{LC} \geq \Delta T \end{aligned} \tag{3}$$

where N_c is the number of collisions detected in a time period and assumes values up to a maximum $N_c^{\max}$, while it is reset to 0 when the time difference from last collision t_{LC} to the current time t_k is greater than a threshold ΔT.

This means, in practice, that RMF has the tendency to fly less aggressively as the number of collisions increase. This in turn offers multiple benefits as the reduced accelerations and the - for the same time - reduced speeds allow the reactive collision-avoidance strategy described in Section IV-B to handle more of the obstacles in the environment, while subsequent collisions take place with reduced kinetic energy and thus represent a lesser challenge for the onboard visual-inertial odometry.

D. Manhole Detection and Navigation

RMF implements a specific mode to enable the autonomous detection and navigation of manhole-sized tubes. First, the robot detects and localizes small manhole openings shaped as rectangles, using the onboard RealSense T265 stereo camera. As T265 provides two monochromatic image sensors with fisheye-lenses, the received image frames are rectified and processed at a framerate of 6FPS. The regions in the rectified images below a darkness threshold are separated and used as a mask, on which morphological operations are performed to remove noise and small dark regions. Additionally, closed contours are detected on the resulting image, which are then checked for their shape and area. Out of these, rectangular contours are selected, and the entrance to the manhole is calculated in the image frame as the center of the selected contour. The disparity values from the rectangular region's periphery are averaged for the given frame and the position of the entrance to the manhole is estimated in $\mathcal{V}$. The manhole entrance's orientation is also computed by calculating the position of the center of each edge. The estimated pose of the entrance is projected into $\mathcal{I}$ using the current odometry of the sensor. Then the average of the pose values calculated from 25 most recent image frames is used as the final estimation by the RMF to enter the manhole. An outline of this procedure is depicted in Figure 4.

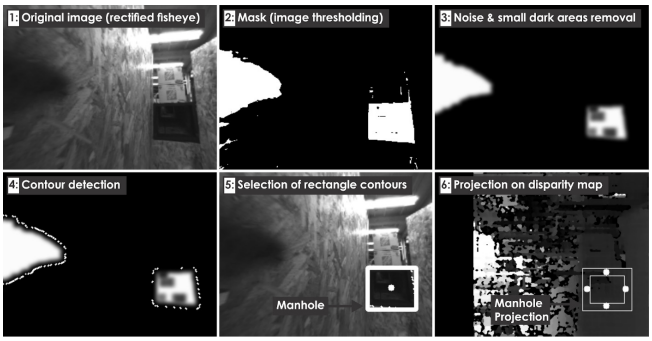

Fig. 4. Processing images to estimate the manhole pose. Rectified images from the sensor (1) are used to create a mask (2). Noise and small regions are removed from the mask (3) and contours are detected (4). Rectangular contours are selected (5), and projected on the disparity map (6).

Provided the capability to detect manholes automatically, RMF implements a particular policy to traverse the extremely constrained passages of manholes both when their geometry is straight and when turning is involved. First of all, due to the extremely constrained environment of a manhole tube, which can lead to the divergence of the position estimation, and the ability of the compliant flaps to self-center the system, the robot disengages the position controller, the reactive avoidance and collisions-aware acceleration adjustments detailed in Sections IV-A, IV-B and IV-C respectively. Instead, a specific manhole navigation mode is triggered once the robot reaches the waypoint right in front of the

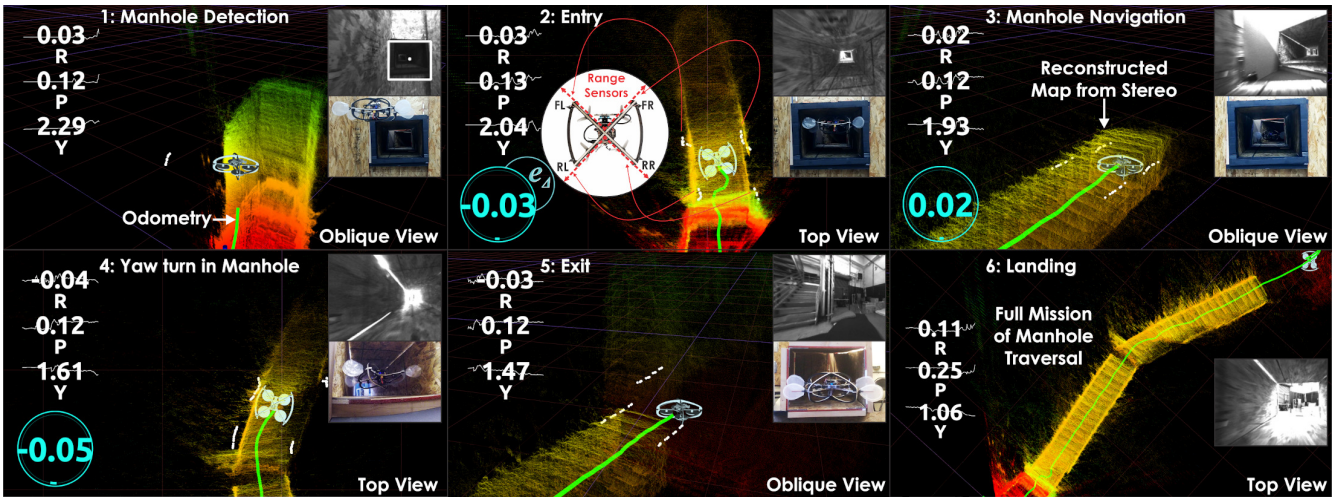

Fig. 5. Instances of an experiment of an autonomous collision-tolerant navigation of a non-straight manhole tube (width $\times$ height $= 0.5 \times 0.4$m) with a total length of 5.2m. RMF resiliently traverses this tight environment by exploiting its compliant flaps which ensure smooth contact with the environment. After a successful detection and localization of the manhole (1), the robot enters the manhole (2) and subsequently "locks" a forward pitch (P) command (3). It minimizes the sum of the left and right diagonals (bottom left turquoise circle) to keep the yaw aligned with the tube (4). Using its TOF sensors, the system is then able to detect the exit of the tube (5) and safely land outside (6). Instances of the mission and of the onboard camera are also presented.

manhole provided by the aforementioned manhole detection and localization process. In particular, once the robot is in front of the manhole it automatically updates its reference waypoint to be slightly inside the manhole and flies to that location, while still under position control. Once all four TOF sensors acquire very close-by readings indicating that the robot entered the manhole completely, then the system "locks" a forward pitch command to fly-through the manhole by commanding a fixed forward acceleration in $\mathcal{V}$, ${}^{\mathcal{V}}a_r^x$, while exploiting its compliant flaps for stability and smooth navigation. As the manhole, or other similar extremely tight space, can involve turnings that are unknown in advance, an additional functionality for heading alignment is implemented utilizing direct TOF sensor data. Considering the relative difference between the sum of distance values returned by the TOF sensors in the left diagonal and right diagonal of the robot $e_\Delta = \delta_{FL} + \delta_{RR} - \delta_{FR} - \delta_{RL}$, the reference yaw rate $\dot{\psi}_r$ is calculated as:

$$\dot{\psi}_r \quad = \quad K_P^{\psi,m} e_\Delta + K_D^{\psi,m} \dot{e}_\Delta \tag{4}$$

This yaw rate reference, constrained in $\pm\dot{\psi}_r^{\max}$, is provided to the low-level autopilot for tracking.

V. EVALUATION STUDIES

To evaluate the resilience and survivability of the proposed Resilient Micro Flyer (RMF) robot design and its collision-aware method for autonomous navigation, a set of challenging experimental studies were conducted. In particular, the presented experiments relate to the following confined navigation tasks: a) the autonomous detection and navigation through a complex manhole with non-straight shape, b) the autonomous safe navigation through a corridor involving multiple obstacles including structurally thin objects, c) the specific evaluation of the effect of adaptive forward control actions in relation to collisions detection, and d) a stress-test of the robustness of the onboard visual-inertial odometry against multiple collisions.

Figure 5 presents the experimental study on autonomous manhole navigation. The robot successfully detects the 0.5×0.4m manhole opening, approaches its entrance and then triggers the manhole navigation mode. As demonstrated, the robot achieves smooth and reliable traversal through this constrained 5.2m-long setting and automatically adjusts its heading to respect the change in manhole shape. The achieved performance is largely attributed to the role of the compliant flaps and the utilization of the TOF sensors for yaw alignment with the manhole shape.

Subsequently, we present a study on resilient navigation of a narrow and obstacle-filled environment by co-exploiting the avoidance strategy of RMF involving its TOF sensors and the collision-aware acceleration adjustment. The result, presented in Figure 6 demonstrates resilient behavior emerging through the combination of avoiding a subset of the obstacles and maintaining safe physical interaction with the environment when complete avoidance was not fully successful either due to the inability of the TOF sensors to detect some objects or due the speed of the movement.

To specifically evaluate the behavior of collision-aware control policy adaptation, we then conducted an experiment involving three intentional collisions with the environment as Figure 7 demonstrates. The system not only sustains all collisions and persists in its navigation task but importantly achieves this behavior by reducing its acceleration commands in response to each collision event. It automatically employs more conservative actions to enhance safety and the likelihood of survival of the onboard estimation process.

Last but not least, we conduct a stress-test of the onboard visual-inertial odometry during collisions, with bumps with a maximum speed up to 1.7 m/s (Figure 8). Due to the ben-

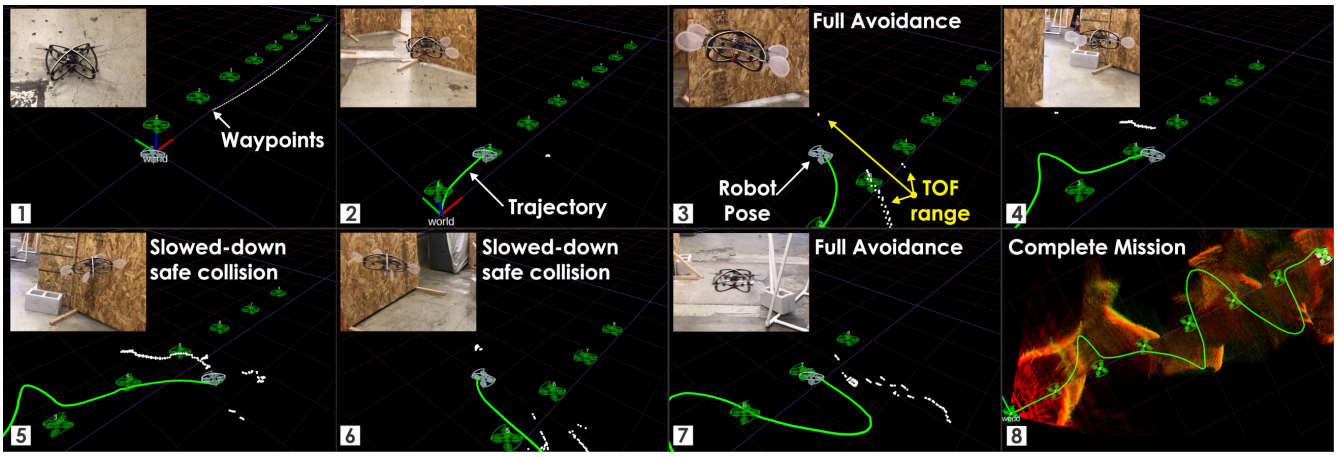

Fig. 6. Instances of an experiment of autonomous resilient navigation of a narrow and obstacle-filled environment by co-exploitation of the avoidance strategy of RMF involving its TOF sensors (3) and the collision-aware acceleration adjustment (5)(6). The obstacles are intentionally placed between the waypoints (8) to demonstrate the reactive behaviour. The combination of these two methods leads to safe navigation and interaction with the environment even when complete avoidance is not fully successful due to the inability of the TOF sensors to detect some objects or the high speed of the movement.

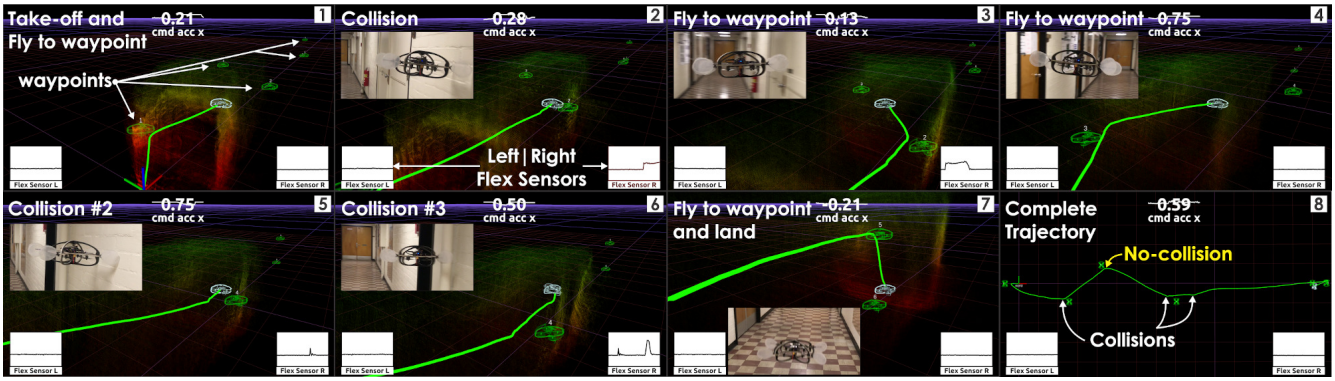

Fig. 7. Instances of an experiment involving three intentional collisions with the environment. RMF is able to sustain all three collisions and to persist in its navigation task by reducing its forward acceleration command (${}^{\mathcal{V}}a_{ad}^{x,a}$) as a reaction to the collision events (2)(5)(6) detected by the integrated flex sensors inside the flaps. This behaviour enhances the safety of the robot and the likelihood of survival of the onboard visual-inertial odometry estimation.

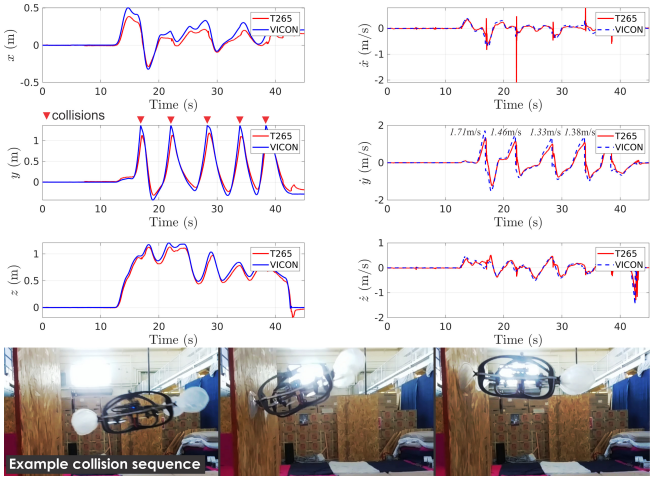

Fig. 8. Results of the stress-test of the onboard visual-inertial odometry. When RMF is equipped with the flaps the VICON ground truth is strictly follwed by the odometry (T265) even after multiple hits with top speed greater than 1.7 m/s.

eficial role of the rigid-compliant design of RMF, primarily through its flaps, the robot maintains reliable pose estimates after a sequence of forceful collisions with the environment. This is an essential property of the robot's design, and it stands at the backbone of its capacity to demonstrate resilient autonomy.

VI. CONCLUSIONS

This paper presented the Resilient Micro Flyer, its system design and collision-tolerance aware navigation strategy. Specifically, the design of the system includes a lightweight rigid frame combined with compliant contact flaps thus offering mechanical robustness and enhancing the survivability of the onboard visual-inertial odometry. A resilient navigation strategy is developed consisting of the position controller combined with a reactive collision avoidance strategy and a collisions-aware adaptive scheme to adjust the forward acceleration of the robot. Furthermore, we develop the detection and navigation policy to allow RMF to traverse narrow manholes. Extensive experimental studies serve to evaluate the proposed system design and navigation solution.

REFERENCES

[1] T. Dang, F. Mascarich, S. Khattak, C. Papachristos, and K. Alexis, "Graph-based path planning for autonomous robotic exploration in subterranean environments," in *2019 IEEE/RSJ International Conference on Intelligent Robots and Systems (IROS)*. IEEE, 2019, pp. 3105–3112.

[2] A. Bircher, M. Kamel, K. Alexis, H. Oleynikova and R. Siegwart, "Receding horizon "next-best-view" planner for 3d exploration," in *IEEE International Conference on Robotics and Automation (ICRA)*, May 2016. [Online]. Available: https://github.com/ethz-asl/nbvplanner

[3] B. Grocholsky, J. Keller, V. Kumar, and G. Pappas, "Cooperative air and ground surveillance," *IEEE Robotics & Automation Magazine*, vol. 13, no. 3, pp. 16–25, 2006.

[4] A. Briod, P. Kornatowski, J.-C. Zufferey, and D. Floreano, "A collision-resilient flying robot," *Journal of Field Robotics*, vol. 31, no. 4, pp. 496–509, 2014.

[5] M. Dharmadhikari, T. Dang, L. Solanka, J. Loje, H. Nguyen, N. Khedekar, and K. Alexis, "Motion primitives-based path planning for fast and agile exploration using aerial robots," in *2020 IEEE International Conference on Robotics and Automation (ICRA)*. IEEE, 2020, pp. 179–185.

[6] K. Alexis, C. Huerzeler, and R. Siegwart, "Hybrid modeling and control of a coaxial unmanned rotorcraft interacting with its environment through contact," in *2013 IEEE International Conference on Robotics and Automation*. IEEE, 2013, pp. 5417–5424.

[7] N. Khedekar, F. Mascarich, C. Papachristos, T. Dang, and K. Alexis, "Contact–based navigation path planning for aerial robots," in *2019 International Conference on Robotics and Automation (ICRA)*, 2019, pp. 4161–4167.

[8] P. De Petris, H. Nguyen, T. Dang, F. Mascarich, and K. Alexis, "Collision-tolerant autonomous navigation through manhole-sized confined environments," in *2020 IEEE International Symposium on Safety, Security, and Rescue Robotics (SSRR)*, 2020, pp. 84–89.

[9] Y. Mulgaonkar, A. Makineni, L. Guerrero-Bonilla, and V. Kumar, "Robust aerial robot swarms without collision avoidance," *IEEE Robotics and Automation Letters*, vol. 3, no. 1, pp. 596–603, 2017.

[10] A. Klaptocz, A. Briod, L. Daler, J.-C. Zufferey, and D. Floreano, "Euler spring collision protection for flying robots," in *2013 IEEE/RSJ International Conference on Intelligent Robots and Systems*. IEEE, 2013, pp. 1886–1892.

[11] A. Briod, A. Klaptocz, J.-C. Zufferey, and D. Floreano, "The airburr: A flying robot that can exploit collisions," in *2012 ICME International Conference on Complex Medical Engineering (CME)*. IEEE, 2012.

[12] A. Klaptocz, G. Boutinard-Rouelle, A. Briod, J.-C. Zufferey, and D. Floreano, "An indoor flying platform with collision robustness and self-recovery," in *2010 IEEE International Conference on Robotics and Automation*. IEEE, 2010, pp. 3349–3354.

[13] Y.-W. Huang, C.-L. Lu, K. Chen, P.-S. Ser, J.-T. Huang, Y.-C. Shen, P.-W. Chen, P.-K. Chang, S.-C. Lee, and H.-C. Wang, "Duckiefloat: a collision-tolerant resource-constrained blimp for long-term autonomy in subterranean environments," *ArXiv*, vol. abs/1910.14275, 2019.

[14] S. Mintchev, S. de Rivaz, and D. Floreano, "Insect-inspired mechanical resilience for multicopters," *IEEE Robotics and automation letters*, vol. 2, no. 3, pp. 1248–1255, 2017.

[15] P. Sareh, P. Chermprayong, M. Emmanuelli, H. Nadeem, and M. Kovac, "Rotorigami: A rotary origami protective system for robotic rotorcraft," *Science Robotics*, vol. 3, no. 22, 2018.

[16] S. Sabet, A. Agha-Mohammadi, A. Tagliabue, D. S. Elliott, and P. E. Nikravesh, "Rollocopter: An energy-aware hybrid aerial-ground mobility for extreme terrains," in *2019 IEEE Aerospace Conference*, 2019, pp. 1–8.

[17] T. Lew, T. Emmei, D. D. Fan, T. Bartlett, A. Santamaria-Navarro, R. Thakker, and A. akbar Agha-mohammadi, "Contact inertial odometry: Collisions are your friend," *ArXiv*, vol. abs/1909.00079, 2019.

[18] D. Gandhi, L. Pinto, and A. Gupta, "Learning to fly by crashing," in *2017 IEEE/RSJ International Conference on Intelligent Robots and Systems (IROS)*. IEEE, 2017, pp. 3948–3955.

[19] D. Floreano and R. J. Wood, "Science, technology and the future of small autonomous drones," *Nature*, vol. 521, no. 7553, 2015.

[20] G. Darivianakis, K. Alexis, M. Burri, and R. Siegwart, "Hybrid predictive control for aerial robotic physical interaction towards inspection operations," in *Robotics and Automation (ICRA), 2014 IEEE International Conference on*, May 2014, pp. 53–58.

[21] H. Hirschmuller, "Stereo processing by semiglobal matching and mutual information," *IEEE Transactions on pattern analysis and machine intelligence*, vol. 30, no. 2, pp. 328–341, 2007.

[22] N. Michael, J. Fink, and V. Kumar, "Cooperative manipulation and transportation with aerial robots," *Autonomous Robots*, vol. 30, pp. 73–86, 2011.